Chapter 1
Concepts and Materials

Solar cells are a promising solution to the energy crisis and environmental pollution. The power conversion efficiencies of classical solar cells are approaching the fundamental limit of 32%. To exceed this limit, new concepts and approaches should been developed. In this chapter, we discuss the energy loss mechanisms in a solar cell and how to avoid these losses using the so-called third generation approaches. Then we focus on photon upconversion. The typical upconversion mechanisms are discussed and an overview of existing upconversion materials is provided. An outline of the thesis is given at the end of the chapter.

1.1 Solar energy and solar cells

The global demand of energy is growing every year while the most important energy resources, the fossil fuels, are decreasing. One of the solutions for this mismatch is to make use of solar energy which is green and renewable. The total amount of solar energy received by earth each second is about 1.74 x 10^{17} W, which is about 1.2 x 10^{4} times more than the average world energy consumption in 2008 (1.50×10^{13} W).[1] If captured effectively, even a small fraction of this energy can meet the rapidly growing energy demand of the world.

To make use of solar energy, we normally need to convert it into other form of energy, such as heat and electricity. Solar cells are devices that generate electricity from sunlight through the photovoltaic effect which was first discovered by Alexandre-Edmond Becquerel in 1839.[2] A typical single junction solar cell is actually a "p-n" junction diode in which photons with energy larger than the band-gap of the active material are absorbed to create electron-hole pairs. These electron-hole pairs are separated to free charge carriers by the "p-n" junction and driven towards the contacts by the built-in potential. When a load is connected to the external circuit, the cell produces both current and voltage.

Solar cells are usually divided into three generations.[3,4] The first generation solar cells is based on crystalline silicon wafers. These solar cells are very efficient, approaching their theoretical maximum of 32% in the laboratory, but the cost of these solar cells is still relatively high. The second generation solar cells are based on thin film technology. They offer lower area production cost, however, their efficiency is lower than that of the first generation solar cells. The third generation solar cells are still under development. The definition of third generation solar cells is that they are high efficiency solar cells made at very low cost. To achieve this goal, new concepts and new materials need to be developed. To date, the third generation approaches include organic solar cells, quantum dot solar cells, multi-junction solar cells, intermediate band solar cells, multiple charge carrier generation solar cells, hot-carrier collection solar cells, and photon upconversion and downconversion solar cells.[3-6] Although at this point the third generation solar cells still face the problem of low stability and very low efficiency, they are

scientifically highly interesting to work on and some of them may be expected to have a bright future, if one or even several of the concepts can be realized successfully.

1.2 Energy lost in a single band-gap solar cell

Figure 1.1 shows the energy loss mechanisms in a single band-gap solar cell.[3] The most significant loss mechanisms in a standard solar cell are due to the incapability of absorbing photons with energy less than the band-gap (process 1 in Figure 1.1) and due to the thermalization of hot charge carriers that are created by photons with energy exceeding the band-gap of the active materials (process 2 in Figure 1.1). These two losses count up to 65% of the total loss in such solar cells. The polychromatic nature of the solar spectrum results in a tradeoff between the two losses. Semiconductors with higher band-gap can reduce energy loss of high energy photons but waste more low energy photons, while low band-gap semiconductors absorb more low energy photons but lose more energy of the high energy photons. So these two loss mechanisms are the fundamental factors that limit the energy conversion efficiency of a single band-gap solar cell. According to a paper published by Shockley and Queisser in 1961, the highest efficiency of a single band-gap solar cell (i.e. under standard solar spectrum illumination) is about 32%.[7]

Other losses in a single band-gap solar cell are the voltage drops across the "p-n" junction and at the contacts (process 3 and 4 in Figure 1.1) and recombination losses of electrons and holes (process 5 in Figure 1.1). Recombination is also an important loss process, but this can be minimized by using materials with high lifetimes of the photogenerated carriers, ensured by minimizing structural defects and impurities.[8]

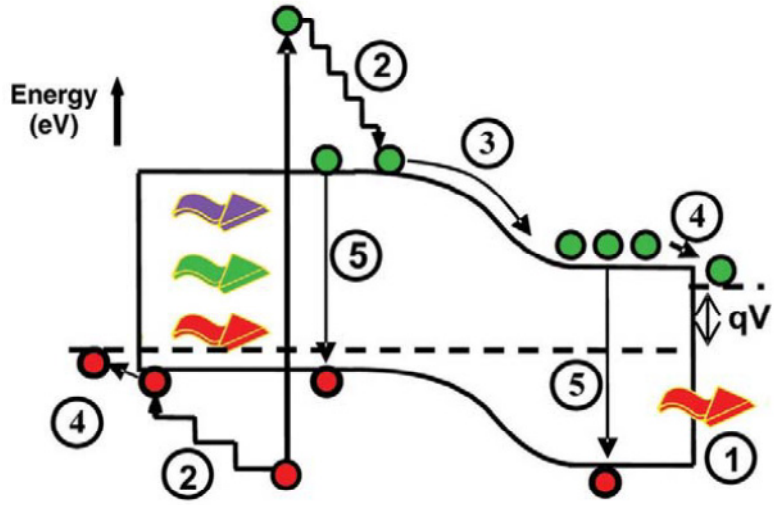

Figure 1.1 *Energy loss processes in a single band-gap solar cell[3]: (1) transmission loss; (2) lattice thermalization loss; (3) and (4) junction and contact voltage losses; (5) recombination loss.*

1.3 Beyond the Shockley-Queisser limit

As indicated above, the key for a solar cell to overpass the Shockley-Queisser limit is to solve the problem of spectral mismatch. To do this, we can either make a solar cell that uses the solar spectrum more efficiently or we can adjust the solar spectrum to better match the absorption spectrum of the solar cell. To date, there are several widely accepted theoretical ways to make a solar cell with a power conversion efficiency beyond the Shockley-Queisser limit. We summarize these most popular possible ways in the next few paragraphs.

1.3.1 Multi-junction solar cells

In a multi-junction solar cell, several "p-n" junctions with different semiconductors of increasing band-gap are placed on top of each other. Each of these junctions absorbs a different section of the solar spectrum, which allows the solar cell to absorb as much energy as possible of the solar spectrum while avoiding thermalization of hot charge carriers. The maximum theoretical limit efficiency of a multi-junction solar cell is up to 86.8%.[9] Currently, the highest

efficiency of multi-junction solar cell has already reached 44.7% for lab samples.[10] Multi-junction solar cells have been studied since 1960s. They are commercial available now. However, the expensive fabrication makes them only suitable for applications where good performance is the only consideration, such as in space.

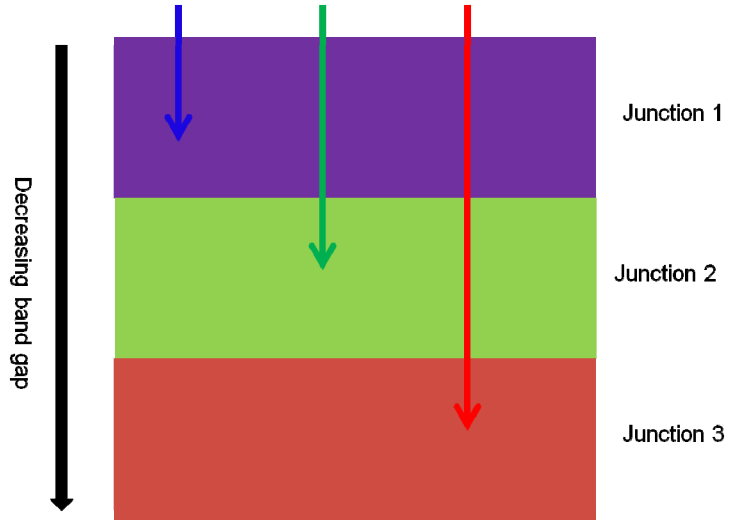

Figure 1.2 *Schematic of a multi-junction solar cell. The arrows indicate photons with different energies being absorbed in the appropriate junction.*

1.3.2 Intermediate-band solar cells

An intermediate band solar cell has an active layer that consists of a semiconductor material that has an intermediate band that is located within the semiconductor band-gap.[11] Since there is an intermediate band in this semiconductor, photons with energy lower than the band-gap of the active material can be absorbed exciting electrons from the valence band to the intermediate band, while other low energy photons can be absorbed exciting electrons further up from the intermediate band to the conduction band. Hence, the cell comprises a kind of two-stage electrical potential pump parallel to the standard semiconductor bandgap, all in one material. Therefore the intermediate band solar cell is able to use more low energy photons without losing much of the excess energy of the high energy photons. Comparing to the multi-junction solar

cells, the theoretical advantage of the intermediate band cell is that in an intermediate cell all charges come out at a single potential, which avoids the difficulties of current matching. Theoretical calculations predict that the efficiency limit of the intermediate band solar cell is 63.2% for a material with ideal band-gap of E_L=0.71 eV (band gap between the valence band and the intermediate band), E_H=1.24 eV (band gap between the intermediate band and the conduction band) and E_G=1.97 eV (semiconductor band gap) under the 6000K black-body spectrum and using maximum sunlight concentration.[12] In reality, however, intermediate band semiconductors are simply unknown.

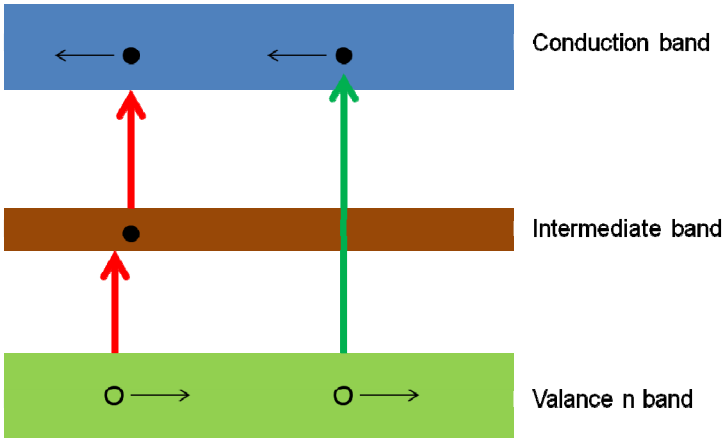

Figure 1.3 *Schematic of an intermediate solar cell.*

1.3.3 Hot carrier solar cells

As described in section 1.2, photons with energy exceeding the band-gap of the active material are absorbed to make hot charge carriers. These hot charge carriers normally lose their excess energy very fast (on picosecond time scale) by relaxing to the band edge and emitting optical phonons. There are two possibilities to prevent this loss.[3,4,13] The first possibility is to collect the hot charge carriers by energy-selective contacts before they have a chance to thermalize. Models show that an ideal hot carrier solar cell made by this concept can reach a power conversion efficiency up to 86% under highly concentrated black body spectrum illumination.[3] However, in reality there is still a very long way to go. Finding suitable absorber

materials which can slow down carrier cooling rates appears highly challenging. To obtain contacts with both good selectivity and high conductivity is difficult, at least.

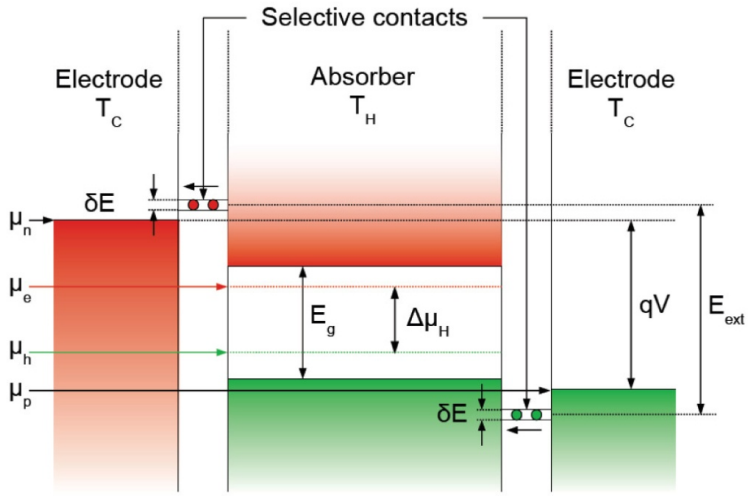

Figure 1.4 *Energy band diagram of a hot-carrier solar cell with bandgap E_g and voltage qV.*[18]

1.3.4 Multiple exciton generation / charge carrier multiplication

Another possibility is to use multiple exciton generation.[14] In some quantum dot semiconductors, such as PbSe[15] and CdSe[16], when the excess energy of a hot charge carrier is greater than (at least) twice the band-gap, one or more additional excitons can be created. Under AM1.5 illumination, the theoretical efficiency of a multiple exciton generation solar cell is up to 44%, if all of the excess band-gap energy leads to the production of extra excitons.[14,17]

1.3.5 Downconversion and upconversion solar cells

All the approaches mentioned above try to achieve higher solar cell efficiencies by better adapting the solar cells to the solar spectrum. The weakness of these approaches is that they either need complicated device structures or require very special materials. Another approach to raise the efficiency of a solar cell beyond the Shockley-Queisser limit is to convert the solar spectrum to a spectrum that is more suitable for the solar cell. This can be done by downconversion or upconversion, in principle (Figure 1.2). Since only the incoming solar

spectrum is modified, it is possible to electrically isolate the up- or down-converters from the active layer and apply them as a separate layer in the solar cells. Hence, adding such a layer to the device structure is feasible for many existing solar technologies.

Downconversion is also known as quantum-cutting.[19] In this process, one incident high energy photon is split by a material into two or more lower energy photons. When the energy of these secondary photons is better matched with the band-gap of the active material, and both are absorbed by the active material, an increase of current in the solar cell is obtained, while the voltage remains the same. Hence, the efficiency of the solar cell is increased. The luminescence downconverter is placed in front of the solar cell, in the standard approach. Trupke *et al.* have calculated the optimum efficiency of a downconversion solar cell as a function of band gap of the active layer material.[20] According to their calculation, the maximum conversion efficiency of 39.6% can be achieved under a 6000K blackbody spectrum when the band gap of the active layer semiconductor is 1.05 eV. This optimum band gap is very close the band gap of crystalline silicon (1.12 eV), which makes downconversion a promising way to increase the efficiency of existing (multi)crystalline silicon solar cells. Although a material with downconversion quantum efficiency close to 200% has been claimed,[21] there is no example of a solar cell with increased efficiency by downconversion, yet.

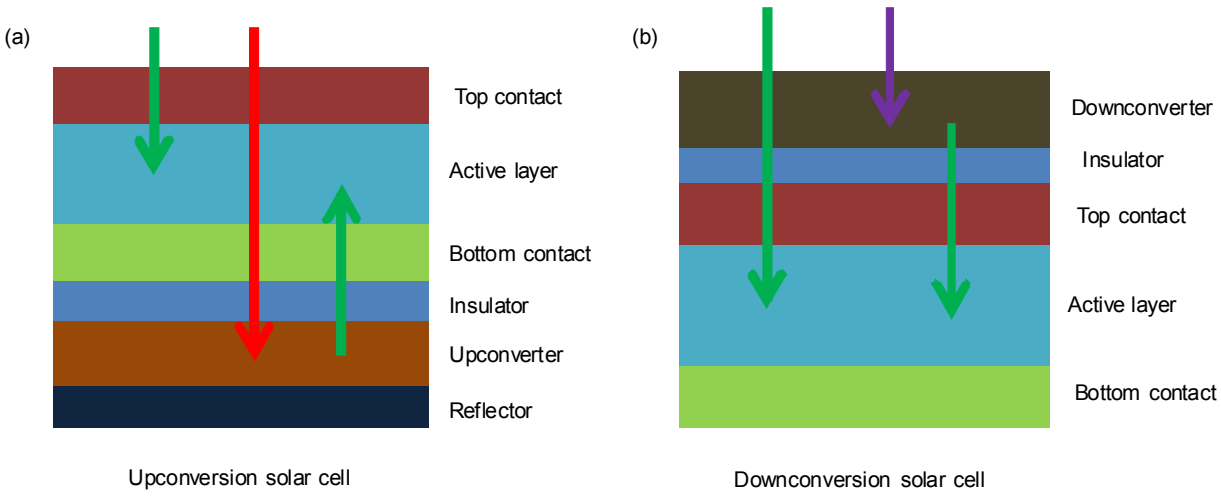

Figure 1.5 *Downconversion and upconversion solar cells.*

Another way to modify the solar spectrum is to use upconversion. Normally in a single band gap solar cell, photons with energy lower than the band gap of the solar cell are lost. For example in a solar cell with a band gap of 2.0 eV, this loss is more than 50% of the total energy from the solar spectrum (Figure 1.6). Upconversion is a process in which two or more low energy photons (sub band gap photons) can be transferred into one high energy photon (i.e. with energy exceeding the band gap). By incorporating upconversion materials into a solar cell, more low energy photons can be harvested, which results an increase of current, increasing the efficiency of the solar cell. The final result of upconversion in solar cell is similar to that of intermediate band solar cell. In both types of cells, a parallel combination of a one-step absorption/charge generation process and a two-step absorption/charge generation process is in operation. The difference between them is that the intermediate band solar cell all processes are to take place inside the photovoltaic active layer, making the realization of an efficient device a formidable challenge, while in the upconversion solar cell the upconverter layer can be electronically isolated from the active cell and located behind it. Therefore, in the upconversion solar cells the active cell and the upconversion layer can be optimized separately to gain optimum efficiency of the solar cell.

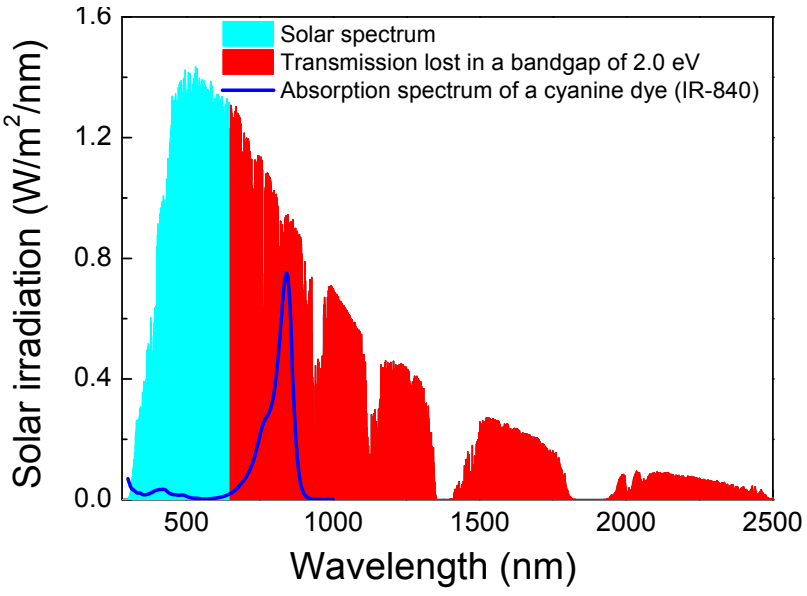

Figure 1.6 *The solar spectrum and the non-absorbed part in a solar cell with a band gap of 2.0 eV (red). The blue line is the absorption spectrum of a cyanine dye IR-840.*

In 2002, Trupke *et al.* have predicted the potential efficiency enhancement of a solar cell due to the application of an upconverter.[22] Their calculations were based on a modified Shockley and Queisser detailed balance model, adding an upconversion layer on the back of the solar cell. As shown in Figure 1.7, they considered an upconverter that has an electronic band structure with a band gap of E_g which ideally matches the band gap of the solar cell. Furthermore, it has an intermediate level E_{IL} with energy E_1 above the valence band and E_2 below the conduction band. Photons with energy larger than the band gap of the solar cell are completely absorbed by the active cell. Photons with energy lower than the band gap are absorbed via two sequential transitions: (1) photons with energy between E_1 and E_2 are completely absorbed via transitions from the valance band to the intermediate band; (2) photons with energy between E_2 and E_g are absorbed to make transitions from the intermediate band to the conduction band of the upconverter. So in their system, three energy ranges of photons can be used by the solar cell. An optimum efficiency of 47.6% is found under non-concentrated 6000K blackbody radiation for a solar cell with E_g = 2 eV, E_1= 0.9393eV and E_2 = 1.3906 eV. Under the standard AM1.5 spectrum, the optimum efficiency can be increased to 50.7% for the same solar cell.

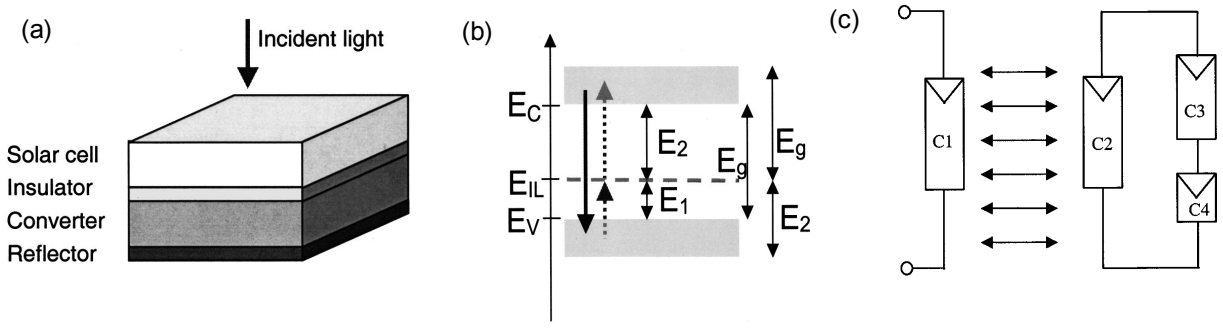

Figure 1.7 *Device structure and energy levels of the upconversion system in the calculation of Trupke et al.[22] (a) A solar cell with an upconversion layer in the back. (b) Energy levels of the upconverter. The dashed line between the valance band and the conduction indicates the intermediate band energy level. (c) Equivalent circuit of the up-conversion system. C1 indicates the active cell. C3 and C4 represent the two intermediate transitions of the upconverter. C2 represents the band-to-band transitions of the upconverter.*

Although the calculations of Trupke *et al.* show a very promising future of using upconversion in solar cells, at this point no materials are able to do the job according to theoretical predictions. However, some proof-of-principle experiments have already been reported for some of the existing upconversion materials. In 1996, Gibart *et al.* first introduced upconversion into a GaAs solar cell.[23] They placed a 100μm thick upconverter layer, made of vitroceramic material, doped with Yb^{3+} and Er^{3+}, on the back of the solar cell. When the solar cell was illuminated using a laser at 1.391 eV (891 nm) with very high excitation density (256 Suns), an efficiency of 2.5% was obtained. Note that 891 nm is not the optimum excitation wavelength for an Yb^{3+} and Er^{3+} co-doped system. When excited at 975 nm wavelength, the efficiency of the solar cell could be much higher. The second example of using upconversion in a solar cell was reported by Shalav *et al.* in 2003.[24] In this example, $NaYF_4$:Er^{3+} up-conversion phosphors were attached to the rear of a bifacial crystalline silicon solar cell, which led to a detectable photoresponse of the solar cell under excitation at 1500 nm. Two years later, Shalav *et al.* published another paper about using $NaYF_4$: 20% Er^{3+} in a bifacial crystalline silicon solar cell.[25] They optimized the incident wavelength and light intensity and found that under 2.4 W/cm^2 1523 nm laser excitation the external quantum efficiency (EQE) of the solar cell was 2.5±0.2%, corresponding to an internal quantum efficiency (IQE) of 3.8%. The same system was also studied by Fischer *et al.* under even lower excitation intensity in 2010.[26] Their solar cell showed an EQE of 0.34% at an irradiance of 0.03 W/cm^2 (1090 W/m^2) at 1522 nm. Goldschmidt et al. applied $NaYF_4$: 20% Er^{3+} to silicon solar cells and investigated the EQE under white light illumination. In the spectral range from 1460 to 1600 nm, an average upconversion efficiency of 1.07 ± 0.13% was obtained.

Efficiency gain by upconversion has also been demonstrated in a-Si:H solar cells[27-29], in dye sensitized solar cells[30-33] and in organic solar cells.[34,35] In 2010, de Wild *et al.* reported the application of an upconverter to an a-Si:H thin film solar cell.[27] They incorporated a relatively very efficient up-converter β-$NaYF_4$:18% Yb^{3+}, 2% Er^{3+} at the back of the solar cell and obtained a photocurrent of 10 $\mu A/cm^2$ after excitation by a 980 nm 10 mW diode laser. Also in 2010, Shan and Demopoulos reported on the application of an Yb^{3+} and Er^{3+} co-doped LaF_3–TiO_2 layer in a dye-sensitized solar cell. Illuminated with a 980 nm fiber laser with extremely high power density (2.9×10^{13} W/m^2), an open-circuit voltage of 0.40 V and short-circuit current

of 0.036 mA was obtained.[30] The first application of an upconverter in an organic solar cell was reported by Wang *et al.* in 2011.[34] They put a separated YF_3:Yb^{3+}, Er $^{3+}$ upconverter layer in front of a P3HT/PCBM solar cell. When the upconverters were excited by a 975 nm laser (25 mW/cm^2), the incident light was upconvertered by the upconverters and absorbed by the solar cell. A resulting photocurrent density of ca. 16.5 $\mu A/cm^2$ was reported.

Although significant progresses have been achieved in the field of upconversion solar cells, the efficiency gain by upconversion is still very limited, especially under standard solar irradiation intensity. New upconverters need to be developed, showing broadband near-IR absorption and a high quantum upconversion efficiency at low excitation density.

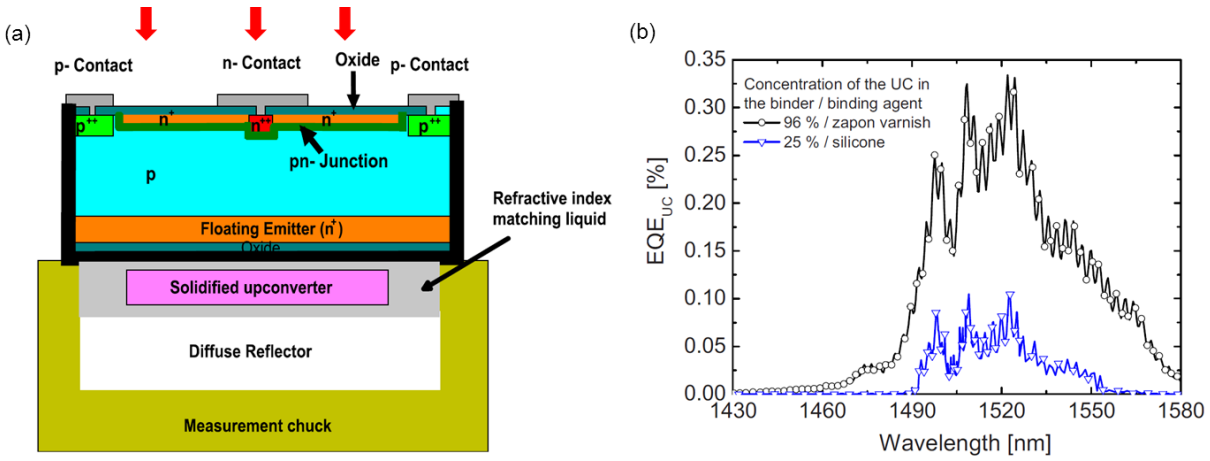

Figure 1.8 *Device structure and EQE response of Fischer's solar cells with $NaYF_4$:Er^{3+} upconverters.*[26]

1.4 Typical upconversion mechanisms

The normal fluorescence behavior follows the principle of Stokes' law by which the exciting photons are of higher energy than the emitted photons. Upconversion is an anti-Stokes processes that usually concerns photons with energies in excess of the excited energies. In these processes, normally two or more low-energy photons are absorbed to emit one high energy

photon. Figure 1.4 shows several well-known processes that convert low-energy photons into higher-energy photons.[36] All these processes are non-linear two photon processes because the power of the output filed scales nonlinearly with the input power (quadratically for two-photon processes in Fig.1.9). Among these processes, second harmonic generation (SHG), and cooperative luminescence processes involve a virtual level, which means that their emission and absorption take place without real electronic levels (Figure 1.3 a, b ,c). Normally these processes need very high excitation intensities and therefore under Sun illumination conditions their efficiencies are very low. The ground state absorption/excited state absorption (GSA/ESA) is the simplest upconversion mechanism (Figure 1.3 e). In the GSA/ESA process, two photons are sequentially absorbed by a single ion, such as Er^{3+}. The first excitation photon absorption results in the population of the intermediate state. If the lifetime of this state is long enough, a second excitation photon can be absorbed to push the electron to a higher exited state. The subsequent relaxation from this excited state to the ground state can be observed as upconversion luminescence. Typical efficiency of this upconversion process is about 10^{-5} cm^2/W.[36] The most efficient upconversion process is the ground state absorption/energy transfer upconversion (GSA/ETU) (Figure 1.3 f). Compared to the GSA/ESA process, GSA/ETU process involves energy transfer which makes it more complex. Generally two types of ions are involved in this process, a sensitizer and an activator. First, two sensitizer ions are excited by absorption of two photons from the ground states. Then they transfer their energies stepwise to the activator ion where the upconversion happens. The sensitizer usually has much stronger absorption than the activator. The efficiency of GSA/ETU process is much higher than that of GSA/ESA, normally on the order of 10^{-3} cm^2/W. Therefore the most useful upconversion materials used for solar cells are the GSA/ETU mechanism materials. The Er^{3+} and Yb^{3+} co-doped systems are most important examples hereof.

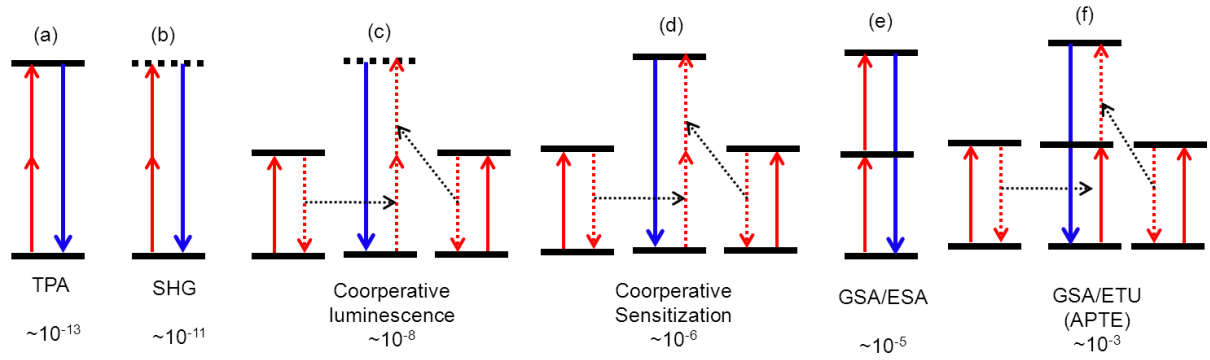

Figure 1.9 *Processes that convert low-energy photons into higher-energy photons. The solid lines indicate the real energy levels while the dashed lines indicate the virtual energy levels. The dashed black arrows indicate the energy transfer between ions. The numbers below the sketches indicate the quantum efficiencies of the processes (in cm^2/W).*[36]

1.5 Power dependence of upconversion luminescence

Upconversion is a non-linear optical process. The intensity of the upconversion emission depends on the intensity of the incident light. In 2000, Pollnau *et al.* analyzed the theoretical dependency of upconversion emission on the excitation power from rate equations for a system containing 3 excited state levels.[37] In his calculation, the following assumptions were made: (1) there is no pump depletion, (2) a constant ground state population, (3) only ESA and ETU upconversion processes are in operation, (4) the decay takes place with rate constants $A_i = t_i^{-1}$, where t_i is the lifetime of the i excited state. The rate equations for the system with 3 excited state levels are shown as following:

For ESA:

$$dN_1/dt = \rho_p \sigma_0 N_0 - \rho_p \sigma_1 N_1 - A_1 N_1 \quad (1)$$

$$dN_2/dt = \rho_p \sigma_1 N_1 - A_2 N_2 \quad (2)$$

For ETU:

$$dN_1/dt = \rho_p \sigma_0 N_0 - 2W_1 N_1^2 - A_1 N_1 \quad (3)$$

$$dN_2/dt = W_1 N_1^2 - A_2 N_2 \quad (4)$$

In the equations, N_0, N_1, and N_2 are the population densities of the ground state, the intermediate state, and the upconversion emitting state, respectively. σ_j is the absorption cross section from state j and W_i is the up-conversion parameter. A_j is the spontaneous emission rate from state i and ρ_p is the pump rate. Solutions to the rate equations for small upconversion and large upconversion are summarized in Table 1.1. In a system, when upconversion is the dominant process, i.e., $N_i \sim P$, the population density of the state where the upconversion happens varies linear with the excited power. When linear decay is the dominant process, i.e., $N_i \sim P^i$, the population density of the state where the upconversion happens varies exponentially with the excitation power.

For most of the existing upconversion materials, the upconversion efficiency is still low and their efficiency is dependent on the excited power, which limits their applications in solar cells.

Influence of upconversion	Upconversion mechanism	Predominant decay route	Fraction of absorbed pump power	Power dependence	From level
(1) small	ETU or ESA	next lower state or ground state	small or large	$N_i \sim P^i$	$i = 1, \ldots, n$
(2) large	(A) ETU	(i) next lower state	small or large	$N_i \sim P^{i/n}$	$i = 1, \ldots, n$
		(ii) ground state	small or large	$N_i \sim P^{i/2}$ $N_i \sim P^1$	$i = 1, \ldots, n\text{-}1$ $i = n$
	(B) ESA	(i) next lower state	(a) small	$N_i \sim P^i$	$i = 1, \ldots, n$
			(b) large	$N_i \sim P^{i/n}$	$i = 1, \ldots, n$
		(ii) ground state	small or large	$N_i \sim P^0$ $N_i \sim P^1$	$i = 1, \ldots, n\text{-}1$ $i = n$

Table 1.1 *Characteristic slopes of the steady-state excited-state population densities N_i of levels i =1,…,n and luminescences from these states for n-photon excitation.*[37]

1.6 Upconversion materials

Upconversion materials are materials that can generate one high-energy photon from absorption of two or more low-energy photons. The concept of upconversion was first proposed by Bloembergen in 1959.[38] In 1966, Auzel observed the upconversion process for the first time[39]. Due to their potential applications in solid state laser,[40] bio-imaging[41] and solar cells,[42]

upconversion materials are becoming a popular research topic. In the past 10 years, the number of publications in this field has increased rapidly. Up to now, there are three main types of upconversion materials: (1) Lanthanide-based upconversion materials, (2) Transition metal-based upconversion materials, and (3) molecular upconversion materials. In this thesis, we introduce dye-sensitized upconversion materials. We will discuss them in detail later. Below, the three existing types of upconversion materials are discussed.

1.6.1 Lanthanide based upconversion materials

Most of the existing upconversion materials are based on Lanthanides (Ln), which are the group of elements with atomic numbers 57 through 71 (La, Ce, Pr, Nd, Pm, Sm, Eu, Gd, Tb, Dy, Ho, Er, Tm,Yb, Lu). The lanthanides usually exist as trivalent ions, in which case their electronic configuration can be written as (Xe) $4f^n$, where n is the number of electrons in the 4*f* shell which varies from 1 (Ce^{3+}) to 14 (Lu^{3+}). The $4f^n$ electronic configuration of a trivalent lanthanide ion gives rise to many energy states, which can be assigned as $^{(2S+1)}L_J$ terms, where S is the total spin angular momentum, L the total orbital angular momentum and J the total angular momentum. The interaction of the 4*f* electrons with a crystal field of a surrounding environment results in further splitting of these levels into Stark levels. In 1960's, Dieke *et al.* have done impressive work in characterization of the $^{(2S+1)}L_J$ energy levels of trivalent lanthanide ions.[43] The energy level diagram resulted from their work is called the "Dieke diagram" in which the allowed optical transitions are plotted as energies for different ions as shown in Figure 1.10. The rich set of energy levels of trivalent lanthanide ions is especially important for the phenomenon of upconversion. The electrons in the partially filled 4*f* shells are shielded from external perturbations by the filled 5*s* and 5*p* orbitals. As a result, they are less sensitive to the chemical environments around the lanthanide ions. And due to this shielding of the *f* electrons, electron–phonon coupling to *f–f* transitions is significantly reduced, which results in slowing down multiphonon relaxation processes. The 4*f* – 4*f* transitions are Laporte-forbidden, resulting in long-lived excited states. These increase the possibilities of processes such as cross-relaxation or upconversion. In principle, upconversion can happen in most lanthanide doped crystalline materials. However, up to now only a few of them (Pr^{3+}, Nd^{3+}, Er^{3+}, Tm^{3+} and Ho^{3+}) show relatively efficient upconversion[36]. Er^{3+} is the first ion showing upconversion and it is the best

active ion for upconversion[39]. Its ground state absorption is at around 1523 nm ($^4I_{15/2}\rightarrow{}^4I_{13/2}$). The long-lived excited states allow energy transfer between two excited ions to yield higher-lying excited states and subsequently emit photons with higher energy. Typical upconversion emission can be observed at around 980 nm ($^4I_{11/2}\rightarrow{}^4I_{15/2}$), 810 nm ($^4I_{9/2}\rightarrow{}^4I_{15/2}$), 660 nm ($^4F_{9/2}\rightarrow{}^4I_{15/2}$) and 550 nm ($^4I_{3/2}\rightarrow{}^4I_{15/2}$).[44] Some of Er^{3+} doped materials that show upconversion properties are listed in Table 4 of reference 39. Since the $4f - 4f$ transitions are Laporte-forbidden, the absorption of lanthanide doped materials is very weak. This strongly limits the practical use of them, especially in solar cells in which strong absorption of light is crucial for obtaining a relevant efficiency. One way to enhance the absorption is to dope the material with another lanthanide ion, serving as sensitizer. This sensitizer should have stronger absorption and it should match the excited states of the activator to ensure efficient energy transfer from the sensitizer to the activator. The most widely used sensitizer to date is the Yb^{3+} ion. The relative intense absorption cross-section at around 975 nm ($^2F_{7/2}\rightarrow{}^2F^{5/2}$) of Yb^{3+} ion matches well with several of the above mentioned ions and it is possible to transfer the energy to these ions by the ETU mechanism. The hexagonal Yb^{3+} and Er^{3+} co-doped $NaYF_4$ is the most efficient upconversion lanthanide material known to date.[45] The upconversion mechanism is shown in Figure 1.11. Yb^{3+} ions are excited from the ground state ($^2F_{7/2}$) to the excited state ($^2F^{5/2}$), by a laser at around 975 nm. Subsequently, two excited Yb^{3+} ions transfer their energy to one Er^{3+} ion step by step and finally the Er^{3+} ion gives the red and green upconversion emission. Due to its relatively high upconversion efficiency, β-$NaYF_4$:Yb,Er has already been used in amorphous silicon solar cells.[27] Currents were detected both upon 980 nm and 1560 nm laser excitation. Another efficient Yb^{3+}-sensitized upconversion material is $NaYF_4$:Yb,Tm which follows a similar upconversion mechanism as $NaYF_4$:Yb,Er. However, the main upconversion emission of Tm^{3+} at about 800 nm. This makes it unsuitable for some solar cells made of large band-gap materials, such as P3HT.

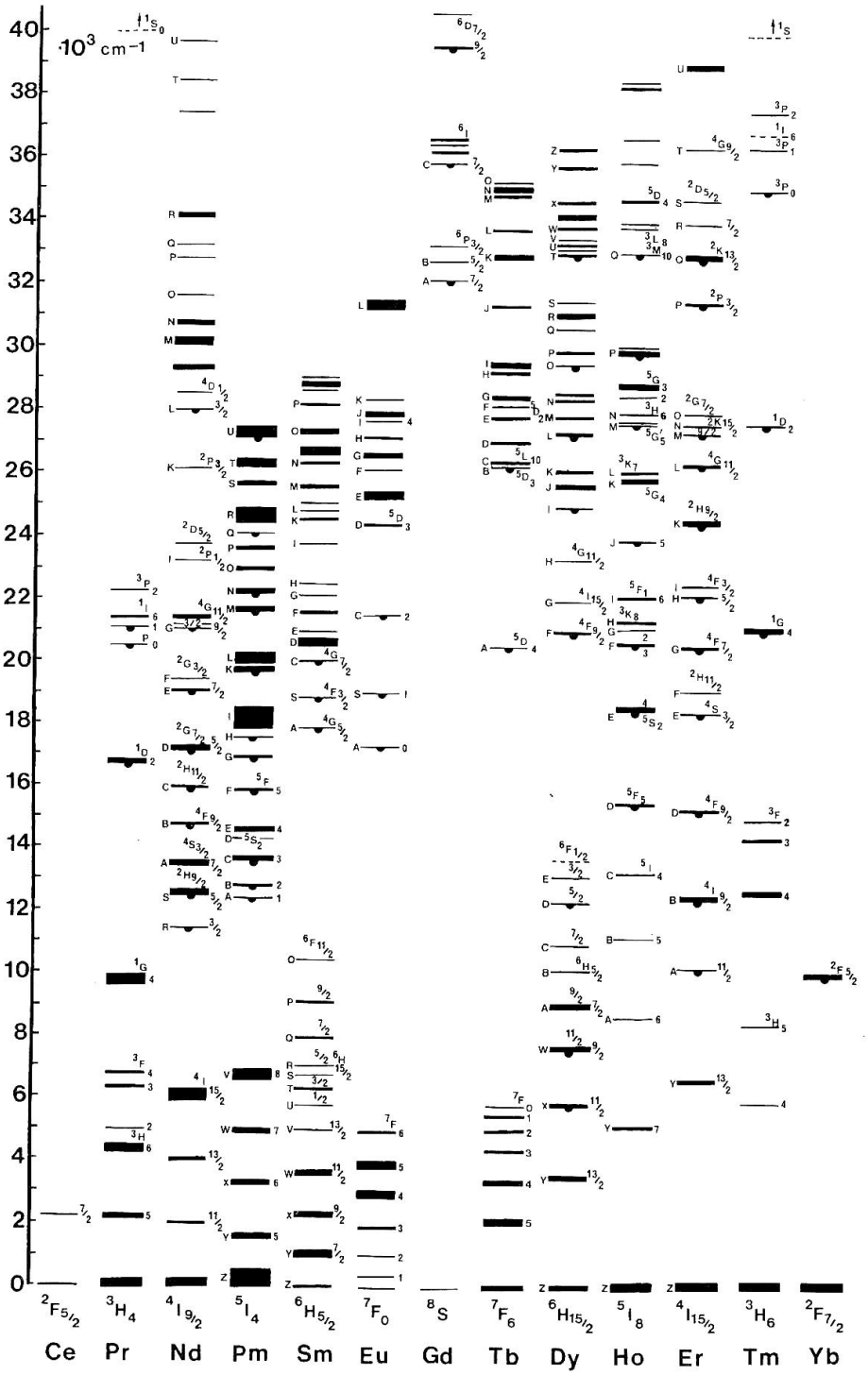

Figure 1.10 *The Dieke diagram of $4f^n$ energy levels of trivalent lanthanide ions.*[43]

When putting the upconverters inside the active layer of organic solar cells, small upconversion nanoparticles are preferable. However, a problem is that the smaller the nanoparticles, the lower the upconversion efficiency.[46] For example, the upconversion efficiency of 100 nm β- $NaYF_4$:Yb,Er nanoparticles is 10 times lower than that of the corresponding bulk material. When the size of the particles is decreased further to 10 nm, the upconversion efficiency becomes 600 times lower than that of bulk material. Several methods have been introduced to enhance the upconversion efficiency of lanthanide doped nanoparticles, such as core-shell structures[45,47] and plasmonic modulation.[48-50] In our study, we enhance the upconversion efficiency of β- $NaYF_4$:Yb,Er nanoparticles by introducing dye-sensitized upconversion in which an organic dye is used as antenna to absorbed more NIR photons and transfer the energy to the nanoparticles. We will discuss it in detail later on in this thesis.

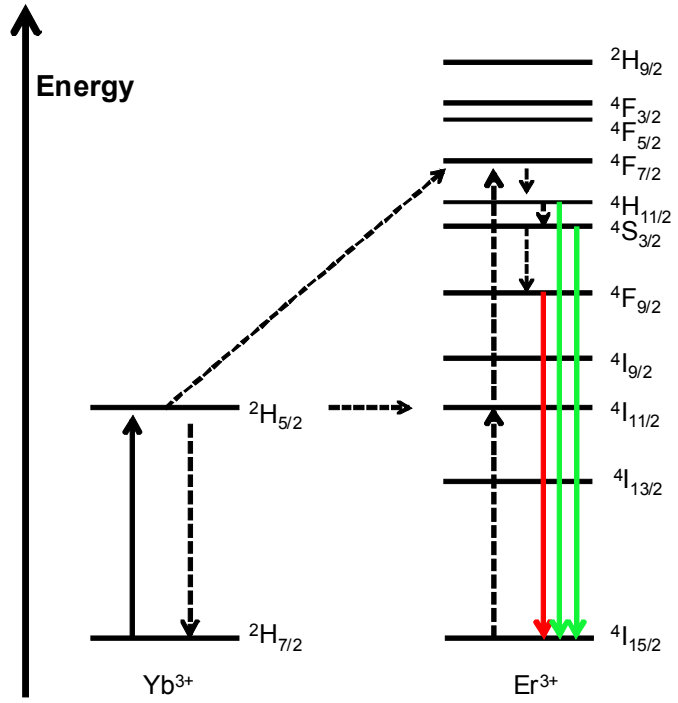

Figure 1.11 *Schematic diagram of upconversion processes of $NaYF_4$:Yb,Er. Solid arrows indicate absorption or emission processes. Dotted arrows indicate energy transfer or multiphonon relaxation processes.*

1.6.2 Transition metal based upconversion materials

The upconversion properties of transition metal ion doped crystalline materials are less studied than those of lanthanide doped materials. Most transition metal ions have only one metastable excited state and therefore most of them are not suitable for upconversion purposes. However, there are a few transition metal ion-doped host materials that show upconversion properties. Examples are Re^{4+}, Ti^{2+}, Os^{4+}, Cr^{3+} and Mo^{3+} ions.[36,51-53] Transition metal ion upconversion originates from transitions of d-electrons. These transitions are sensitive to the type of host materials. Compared to lanthanide-doped upconversion materials, the advantage of transition metal ion-doped upconversion materials is that they have higher absorption oscillator strengths and broad band absorption and emission abilities. This makes them much more versatile for application in solar cells. However, up to now, there is only one transition metal doped material (Cs_2ZrCl_6 : Re_4)[54,55]showing upconversion at room temperature. All other examples only show upconversion at very low temperatures.

1.6.3 Organic upconversion materials

Upconversion can also be obtained from organic molecules. Although the first example has been reported by Parker *et al.* as early as in the 1960s,[56] the research field remained small until only a few years ago. Typically, the upconverter consists of a sensitizer (usually an organometallic complex) and acceptor (a π-conjugated organic molecule).[57] The typical upconversion mechanism is shown in Figure 1.12. First, upon absorption of a photon, the sensitizer is excited from the ground state (S_0) to the lowest singlet excited state (S_1). Assisted by the heavy transition metal ion through spin-orbit coupling, the singlet excited state relaxes through intersystem crossing to the triplet excited state (T_1). When the lifetime of the triplet excited state is long enough, the triplet state energy can be transferred to the acceptor, resulting in triplet excited acceptor. Subsequently, two triplet excited acceptor molecules can annihilate, resulting in one singlet excited acceptor molecule. Finally, the singlet excited acceptor can emit a photon with higher energy than that of the individual originally absorbed photons. To obtain efficient upconversion emission, the energy gap between the S_1 and T_1 states of the acceptor

should be as large as possible while the gap between the S_1 and T_1 excited states of the sensitizer should be as small as possible.

For application in solar cells, the main advantage of organic upconverters is their strong broadband absorption and their relatively high efficiency at low excitation intensity. Upconversion has been observed with excitation power as low as a few mW/cm^2, lower than the unfocused solar irradiance (100 mW/cm^2). An upconversion efficiency of 18.1% (excited at 445 nm, emit at 410 nm) has been obtained in a system with Platinum(II) Bis(arylacetylide) complexes as sensitizer and 9,10-diphenylanthracene (DPA) as acceptor.[60] The present drawback of molecular upconverters for application in solar cells is that the absorption range of these materials is usually limited to 650–750 nm, at present,[56-59] while common solar cells themselves absorb light at longer wavelength. Hence, relevant PV upconversion is in the range 800-2000 nm. To ensure efficient energy transfer from the sensitizer to the acceptor, the distance between the sensitizer and the acceptor should be as small as possible, which may limits the application of them. For example, when the donor and acceptor are added to an active layer of a polymer solar cell, the can be separated by the polymer to a long distance, resulting low efficient energy transfer between the donor and acceptor.

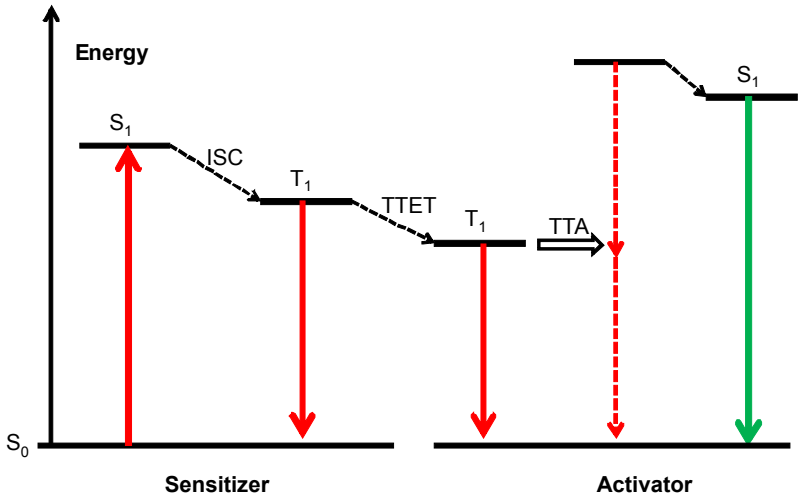

Figure 1.12 *Mechanism of TTA upconversion process illustrated in a Jablonski Diagram. Solid arrows indicate absorption or emission processes. Dotted arrows indicate energy transfer or triplet to triplet annihilation processes. Figure modified from reference 57.*

1.7 Summary and outline

Due to fundamental constrains, a large part of energy in the solar spectrum is lost in a standard single band gap solar cell, which results in the Shockley-Queisser limit of 32% for a single-junction solar cell. Upconversion, in which low energy photons are transferred into high energy photons, is considered as a promising way for a single band gap solar cell to overpass the Shockley-Queisser limit. At the start of this Chapter, we discussed the energy loss mechanisms in a solar cell and the so-called third generation approaches to surpass the Shockley-Queisser limit. We focus on the potential use of upconversion in solar cells in our study. The typical upconversion mechanisms were discussed and an overview of existing upconversion materials was given at the end of the Chapter.

β-$NaYF_4$:Yb,Er is the most efficient upconversion material. The application of its nanoparticles in amorphous silicon solar cells has been reported.[27] However, up to now, application in organic solar cells has not been studied. In Chapter 2, we describe the synthesis of β-$NaYF_4$:Yb,Er nanoparticles with an average size of 16 nm. We mix these nanoparticles with the P3HT/PCBM blend and we optimize the morphology of the film. We show that a considerable concentration of nanoparticles in the film has little impact on the absorption of the film while significantly enhancing the emission of the polymer. We also show that there is energy transfer from the nanoparticles to the polymer. However, we did not detect any increment of photocurrent when the nanoparticles were added to the active layer of the solar cells.

Up to now, the upconversion solar cell efficiencies obtained experimentally have been extremely low and merely serve as proof of principle. The main problem is that the known internally efficient upconversion materials absorb extremely weakly and within a very narrow spectral window. In our study, we focus on using organic NIR dyes as antenna to increase and broaden the absorption of the nanoparticles. In Chapter 3, we show the syntheses and characteristics of suitable organic dyes.

In Chapter 4, we show the concept of dye-sensitized upconversion. We attach an organic dye to the β-$NaYF_4$:Yb,Er nanoparticles and we study the upconversion properties of the product. We show that the energy absorbed by the organic dyes is transferred to the nanoparticles. Due to

the strong and broad absorption of the organic dyes, the overall upconversion of the dye-sensitized nanoparticles is dramatically enhanced by a factor of 3300. The upconversion intensity of the nanoparticles is dependent on the concentration of the organic dyes. The power dependence measurement shows that the upconversion is a two photon process.

It is difficult to cover the whole NIR range of the solar spectrum through absorption by a single type of dye molecule. In Chapter 5, we show the concept of co-sensitized upconversion. We attach two organic dyes with different absorption range to the same nanoparticle to absorb a broader range of NIR light. We show that the optimized overall upconversion efficiency is about 20% higher as a result of co-sensitization.

1.8 References

1. *Statistical Review of World Energy*, **2009**. [http://www.bp.com]
2. Becquere, A. E. Diagram of apparatus described by Becquerel. *C.R. Acad. Sci.* **1839**, *9*, 145&561.
3. Conibeer, G. Third-generation photovoltaics. *Mater. Today* **2007**, *10*, 42–50; Van der Ende, B. M., Aarts, L. & Meijerink, A. Lanthanide ions as spectral converters for solar cells. Phys. Chem. Chem. Phys. 2009, 11, 11081–11095.
4. Green, M. A. *Third-generation photovoltaics: advanced solar energy conversion.* Springer, **2006.**
5. Li, G., Zhu, R., Yang, Y. Polymer solar cells. *Nature Photon.* **2012**, *6*, 153–161.
6. Kamat, P. V. Quantum dot solar cells. Semiconductor nanocrystals as light harvesters. *J. Phys. Chem. C.* **2008**,*112*, 18737–18753.
7. Shockley, W., Queisser, H. J. Detailed balance limit of efficiency of p-n junction solar cells. *J. Appl. Phys.* **1961**, *32*, 510–519.
8. Green, M. A. Third generation photovoltaics: solar cells for 2020 and beyond. *Physica E* **2002**, *14*, 65-70.
9. Marti, A., Araujo, G. L. Limiting efficiencies for photovoltaic energy conversion in multigap systems. *Sol. Energy Mater. Sol. Cells* **1996**, *43*, 203.

10. Dimroth, F. Wafer bonded four-junction GaInP/GaAs/GaInAsP/GaInAs concentrator solar cells with 44.7% efficiency. *Prog. Photovolt. Res. Appl.* 2014, **22**, 277–282.
11. Luque, A., Marti, Q., Stanley, C. Understanding intermediate-band solar cells. *Nature Photon.* **2012**, *6*, 146-152.
12. Luque, A., Mart, A. Increasing the efficiency of ideal solar cells by photon induced transitions at intermediate levels. *Phys. Rev. Lett.* **1997**, *78*, 5014-5016.
13. Wurfel1, P., Brown, A. S., Humphrey, T. E., Green, M. A. Particle conservation in the hot-carrier solar cell. *Prog. Photovolt: Res. Appl.* **2005**, *13*, 277–285
14. Nozik, A. J. Multiple exciton generation in semiconductor quantum dots. *Chemical Physics Letters* 2008, 457, 3–11.
15. Pijpers, J. J. H., Ulbricht, R., Tielrooij, K. J., Osherov, A., Golan, Y., Delerue, C., Allan, G., Bonn, M. Assessment of carrier-multiplication efficiency in bulk PbSe and PbS. *Nature Physics* **2009**, *5*, 811–814.
16. Schaller, R., Agranovich, V. M., Klimov, V. I. High-efficiency carrier multiplication through direct photogeneration of multi-excitons via virtual single-exciton states. *Nature Physics* **2005**, 1, 189–194.
17. Hanna, M. Nozik, A. Efficiency of photovoltaic and photoelectrolysis cells with carrier multiplication absorbers. *J. Appl. Phys.* **2006**, *100*, 074510.
18. Bris, A. L. *et al.*, Hot carrier solar cells: In the making? *25th European Photovoltaic Solar Energy Conference and Exhibition 5th World Conference on Photovoltaic Energy Conversion*, Valencia, Spain, **2010**, 683–685.
19. Oskam, K. D., Wegh, R. T., Donker, H., Loef, van E. V. D.， Meijerink, A. Downconversion: a new route to visible quantum cutting. *Journal of Alloys and Compounds* **2000**, *300–301*, 421–425.
20. Trupke, T., Green, M. A., Würfel, P. Improving solar cell efficiencies by down-conversion of high-energy photons. *J. Appl. Phys.* **2002**, *92*, 1668.
21. Justel, T., Nikol, H., Ronda, C. New developments in the field of luminescent materials for lighting and displays. *Angew. Chem. Int. Ed.* **1998**, *37*, 3084 –3103.
22. Trupke, T., Green, M. A., Würfel, P. Improving solar cell efficiencies by up-conversion of sub-band-gap light. *J. Appl. Phys.* **2002**, *92*, 4117.

23. Gibart, P., Auzel, F., Guillaume, J. C., Zahraman, K. Below band-gap IR response of substrate-Free GaAs solar cells using two-photon up-conversion. *J. Appl. Phys.* **1996**, *35*, 4401.

24. Shalav, A., Richards, B. S., Trupke, T., Corkish, R. P., Gäme, K. W., Güdel, H. U. Green, M. A. The applications of up-converting phosphors for increased solar cell conversion efficiencies. *IEEE Proc.3rd World Conf. on Photovoltaic Energy Conversion*, Osaka, Japan, **2003**, *1P-D3–25*, 248–250.

25. Shalav, A., Richards, B., Trupke, T., Krämer, K., Güdel, H. Application of $NaYF_4:Er^{3+}$ up-converting phosphors for enhanced near-infrared silicon solar cell response. *Appl. Phys.Lett.* **2005,** *86,* 013505.

26. Fischer, S. *et al*. Enhancement of silicon solar cell efficiency by upconversion: Optical and electrical characterization. *J. Appl. Phys.* **2010**, *108*, 044912.

27. De Wild, J., Rath, J. K., Meijerink, A., Van Sark, W. G. J. H. M., Schropp, R. E. I. Enhanced near-infrared response of a-Si:H solar cells with β-$NaYF_4:Yb^{3+}$ (18%), Er^{3+} (2%) upconversion phosphors. *Solar Energy Materials and Solar Cells* **2010**, *94*, 2395–2398.

28. Chen, Y. *et al*. β-$NaYF_4:Er^{3+}$(10%) microprisms for the enhancement of a-Si:H solar cell near-infrared responses. *Journal of Luminescence* **2012**, *132*, 2247–2250.

29. De Wild, J. et al. Increased upconversion response in a-Si:H solar cells with broad-band light. *IEEE J. Photovoltaics* **2013**, *3(1)*, 17-21.

30. Shan, G. B., Demopoulos, G. P. Near-infrared sunlight harvesting in dye-sensitized solar cells via the insertion of an upconverter-TiO_2 nanocomposite layer. *Adv. Mater.* **2010**, *22*, 4373–4377.

31. Chang, j., Ning, Y., Wu, S., Niu W., Zhang, S. Effectively utilizing NIR light using direct electron injection from up-conversion nanoparticles to the TiO_2 photoanode in dye-sensitized solar cells. *Adv. Funct. Mater.* **2013**, *23*, 5910–5915.

32. Yu, J. et al. Er^{3+} and Yb^{3+} co-doped $TiO_{2-x}F_x$ up-conversion luminescence powder as a light scattering layer with enhanced performance in dye sensitized solar cells. *J. Power Sources* **2013**, *243*, 436–443.

33. Liang, L. et al. Highly uniform, bifunctional core/double-shell-structured β-$NaYF_4:Er^{3+}$, Yb^{3+} @ SiO_2@TiO_2 hexagonal sub-microprisms for high-performance dye-sensitized solar cells. *Adv. Mater.* **2013**, *25*, 2174–2180.

34. Wang, H. Q., Stubhan, T., Osvet, A., Litzov, I., Brabec, C. J. Up-conversion semiconducting MoO3:Yb/Er nanocomposites as buffer layer in organic solar cells. *Sol. Energy Mater. & Sol. Cells* **2012**, *105*,196–201.
35. Kong, M. et al. Efficiency enhancement in P3HT-based polymer solar cells with a $NaYF_4$:2% Er^{3+}, 18% Yb^{3+} up-converter. *J. Mater. Chem. C.* **2013**, *1*, 5872-5878.
36. Auzel, F. Upconversion and anti-stokes processes with *f* and *d* ions in solids. *Chem. Rev.* **2004**, *104*, 139–173; Etchart I. Metal oxides for efficient infrared to visible upconversion. PhD thesis, University of Cambridge, 2011.
37. Pollnau, M., Gamelin, D. R., Luthi, S. R., Gudel, H. U. Power dependence of upconversion luminescence in lanthanide and transition-metal-ion systems. *Phys. Rev. B* **2000**, *61*, 3337–3346.
38. Bloembergen, N. Solid State Infrared Quantum Counters. *Phys. Rev. Lett.* **1959**, *2*, 84–85.
39. Auzel, F. Computeur quantique par transfert d'energie entre deux ions de terres reres dans un tungstate mixte et dans un verre. *C.R. Acad. SCi.* Paris, **1966**, *262*, 1016–1019; Auzel, F. Computeur quantique par transfert d'energie entre de Yb^{3+} a Tm^{3+} dans un tungstate mixte et dans verre germinate. *C.R. Acad. SCi.* Paris, **1966**, *263*, 819–821.
40. Bowman, S. R., Shaw, L. B., Feldman, B. J., Ganem, J. Spectroscopy of mid-infrared (2.9 μm) fluorescence and energy transfer in Dy^{3+}-doped tellurite glasses. *IEEE journal of quantum electronics* **1996**, *32*, 646-649.
41. Haase, M., Schafer, H. Upconverting nanoparticles. *Angew. Chem. Int. Ed.* **2011**, *50*, 5808–5829.
42. Wang, H. Q., Batentschuk, M., Osvet, A., Pinna, L., Brabec, C. J. Rare-earth ion doped up-conversion materials for photovoltaic applications. *Adv. Mater.* **2011**, *23*, 2675–2680; Van der Ende, B. M., Aarts, L., Meijerink, A., Lanthanide ions as spectral converters for solar cells. Phys. Chem. Chem. Phys. **2009**, *11*, 1081–11095; De Wild, J., Meijerink, A., Rath, J. K., van Sark, W. G. J. H. M., Schropp, R. E. I. Upconverter solar cells: materials and applications. *Energy Environ. Sci.* **2011**, *4*, 4835–4848.
43. Dieke, G. Spectra and energy levels of rare earth ions in crystals. Interscience Publishers New York, **1968**.
44. Strümpel, C. *et al*. Modifying the solar spectrum to enhance silicon solar cell efficiency–An overview of available materials, *Sol. Energy Mater. Sol. Cells* **2007**, *91*,238–249.

45. Yi, G. S., Chow, G. M. Water-soluble $NaYF_4$:Yb,Er(Tm)/$NaYF_4$/polymer core/shell/shell nanoparticles with significant enhancement of upconversion fluorescence. *Chem. Mater.* **2007**, *19*, 341–343.
46. Boyer, J. C., van Veggel, F. C. J. M. Absolute quantum yield measurements of colloidal $NaYF_4$: Er^{3+}, Yb^{3+} upconverting nanoparticles. *Nanoscale*, **2010**, *2*, 1417–1419.
47. Vetrone, F., Naccache, R., Mahalingam, V., Morgan, C. G., Capobianco, J. A. The active-core/active-shell approach: A strategy to enhance the upconversion luminescence in lanthanide-doped nanoparticles. *Adv. Funct. Mater.* **2009**, *19*, 2924–2929.
48. Verhagen, E., Kuipers, L., Polman, A. enhanced nonlinear optical effects with a tapered plasmonic waveguide. *Nano Lett.* **2007**, *7*, 334–337.
49. Rai, V. K. *et al*. Surface-plasmon-enhanced frequency upconversion in Pr^{3+} doped tellurium-oxide glasses containing silver nanoparticles. *J. Appl. Phys.* **2008**, *103*, 093526.
50. Kassab, L. R. P. *et al*. Energy transfer and frequency upconversion in Yb^{3+}-Er^{3+}-doped PbO-GeO2 glass containing silver nanoparticles. *Appl. Phys.* **2009**, *B94*, 239–242.
51. Gamelin, D. R., Gudel, H. U. Upconversion processes in transition metal and rare earth metal systems. *Topics in Current Chemistry* **2000**, *214*, 1–56.
52. Suyver, J. F. *et al*. Novel materials doped with trivalent lanthanides and transition metal ions showing near-infrared to visible photon upconversion. *Optical Materials* **2005**, *27*, 1111–1130.
53. Wenger, O. S., Wermuth, M., Güdel, H. U. Chemical tuning of transition metal upconversion properties. *Journal of Alloys and Compounds* **2002**, *341*, 342–348.
54. Gamelin, D. R., Güdel, H. U. Spectroscopy and dynamics of Re^{4+} near-IR-to-visible luminescence upconversion. *Inorg. Chem.* **1999**, *38*, 5154–5164.
55. Wermuth, M., Güdel, H. U. Luminescence spectroscopy and NIR to VIS upconversion of Cs_2GeF_6: 2% Re^{4+}. *J. Phys.: Condens. Matter* **2001**, *13*, 9583–9598.
56. Singh-Rachford, T. N., Castellano, F.N. Photon upconversion based on sensitized triplet–triplet annihilation. *Coord. Chem. Rev.* **2010**, *254*, 2560–2573.
57. Zhao, J., Ji, S., Guo, H. Triplet–triplet annihilation based upconversion: from triplet sensitizers and triplet acceptors to upconversion quantum yields. *RSC Advances*, **2011**, *1*, 937–950.
58. Cheng, Y. Y. et al. Improving the light-harvesting of amorphous silicon solar cells with

photochemical upconversion. *Energy Environ. Sci.* **2012**, *5*, 6953–6959.

59. Nattestad, A. et al. Dye-sensitized solar cell with integrated triplet−triplet annihilation upconversion system. *J. Phys. Chem. Lett.* **2013**, *4*, 2073−2078.
60. Ji, S. *et al*. Efficient triplet–triplet annihilation upconversion with platinum(II) bis(arylacetylide) complexes that show long-lived triplet excited states. *Eur. J. Inorg. Chem.* **2012**, 3183–3190.